PROCEEDINGS OF SPIE

SPIEDigitalLibrary.org/conference-proceedings-of-spie

Global sensitivity analysis of fractional-order viscoelasticity models

Paul R. Miles, Graham T. Pash, Ralph C. Smith, William S. Oates

Paul R. Miles, Graham T. Pash, Ralph C. Smith, William S. Oates, "Global sensitivity analysis of fractional-order viscoelasticity models," Proc. SPIE 10968, Behavior and Mechanics of Multifunctional Materials XIII, 1096806 (29 March 2019); doi: 10.1117/12.2514160



Event: SPIE Smart Structures + Nondestructive Evaluation, 2019, Denver, Colorado, United States

Global Sensitivity Analysis of Fractional-Order Viscoelasticity Models

Paul R. Miles^a, Graham T. Pash^{a,b}, Ralph C. Smith^a and William S. Oates^c

^aDepartment of Mathematics North Carolina State University Raleigh, NC 27695

^bDepartment of Mechanical Engineering North Carolina State University Raleigh, NC 27695

^cFlorida Center for Advanced Aero Propulsion
 Department of Mechanical Engineering

 Florida A&M University and Florida State University
 Tallahassee, FL 32311

ABSTRACT

In this paper, we investigate hyperelastic and viscoelastic model parameters using Global Sensitivity Analysis (GSA). These models are used to characterize the physical response of many soft-elastomers, which are used in a wide variety of smart material applications. Recent research has shown the effectiveness of using fractional-order calculus operators in modeling the viscoelastic response. The GSA is performed using parameter subset selection (PSS), which quantifies the relative parameter contributions to the linear and nonlinear, fractional-order viscoelastic models. Calibration has been performed to quantify the model parameter uncertainty; however, this analysis has led to questions regarding parameter sensitivity and whether or not the parameters can be uniquely identified given the available data. By performing GSA we can determine which parameters are most influential in the model, and fix non-influential parameters at a nominal value. The model calibration can then be performed to quantify the uncertainty of the influential parameters.

Keywords: Viscoelasticity, Global Sensitivity Analysis, Fractional-Order Calculus

1. INTRODUCTION

Many adaptive structures require accurate estimation of the underlying material's viscoelastic behavior. The nature of the viscoelastic response presents many modeling challenges as the stress response can vary significantly with changes in deformation rate. Extensive research has been done in this field;^{1,2} however, accurately predicting this rate-dependent phenomenon continues to pose a significant challenge. Recent research has shown the viability of using fractional-order operators in describing viscoelastic behavior.³ Fractional-order operators present interesting numerical difficulties, but efficient methods make sampling based model analysis feasible.⁴

Sensitivity analysis is a key component of performing parameter estimation. In many models, the parameters do not play a significant role in the overall behavior of the system, making them difficult to estimate using measured data. Global Sensitivity Analysis (GSA) serves as a tool of identifying how uncertainties in the model output can be apportioned to uncertainties in the input model parameters.⁵ Based on the results obtained from the GSA, parameter estimation can be performed on the remaining sensitive parameters. In many cases, the GSA may find that all model parameters significantly impact the model output; however, that does not mean one will

Further author information: (Send correspondence to P.M.) P.M.: E-mail: prmiles@ncsu.edu, Telephone: 1-919-515-0682

Behavior and Mechanics of Multifunctional Materials XIII, edited by Hani E. Naguib, Proc. of SPIE Vol. 10968, 1096806 \cdot © 2019 SPIE \cdot CCC code: 0277-786X/19/\$18 \cdot doi: 10.1117/12.2514160

necessarily be able to uniquely identify their parameter distributions when performing estimation. By assuming the model parameters are random variables, it is natural to approach the parameter estimation problem from a Bayesian perspective. This enables us to use Markov Chain Monte Carlo (MCMC) methods, which will provide us with an estimate for the parameter posterior densities.

The remainder of this paper is presented in the following sections. The key thermodynamic relations and theory that describe the hyperelastic and viscoelastic models are summarized in Section 2. The methods and results of our sensitivity analysis are outlined in Section 3. Preliminary model calibration is discussed in Section 4, and concluding remarks are provided in Section 5.

2. THEORY

The modeling framework behind this approach has been discussed extensively in,^{3,6} but we include a few key model components for reference. We develop a model to calculate the nominal stress response within the material for comparisons with the experimental measurements. The work conjugate variable to the deformation gradient is the nominal stress,⁷ so we begin by defining an energy density function to relate these variables. The thermodynamic framework for the energy function is generalized by including thermal effects, but the analysis and model validation will assume isothermal deformation. The total energy density function per reference volume is given by

$$\psi = \psi_{\infty}(F_{iK}, \Theta) + \Upsilon(F_{iK}, \Theta, \xi_{iK}^{\nu}). \tag{1}$$

The energy is split into two distinct components: ψ_{∞} is the conserved, hyperelastic free energy function and Υ is an energy function that depends on a non-conserved tensor order parameter. The hyperelastic model depends on the deformation gradient F_{iK} and temperature Θ while Υ is also a function of a set of internal variables, ξ_{iK}^{ν} ($\nu=1,\ldots,n$ non-measurable internal states). These internal states contribute to the dissipation observed during rate-dependent deformation.

A correction term is added to (1) to account for incompressible deformation, which is typical of elastomers. The total free energy density is then

$$\hat{\psi} = \psi - p(J-1),\tag{2}$$

where p is the unknown Lagrange multiplier, which represents a hydrostatic stress and $J = \det(F_{iK})$. Incompressible deformation is thus described by J = 1.

The nominal stress is found by taking the derivative of the total energy density with respect to the deformation gradient,

$$s_{iK} = \frac{\partial \hat{\psi}}{\partial F_{iK}} = \frac{\partial \psi_{\infty}}{\partial F_{iK}} - pJH_{iK} + \frac{\partial \Upsilon}{\partial F_{iK}},\tag{3}$$

where we have used the identity $\partial s \frac{\partial J}{\partial F_{iK}} = J H_{iK}$ and $H_{iK} F_{jK} = \delta_{ij}$. Similarly, the viscoelastic stress is found by taking the derivative with respect to the internal state variable, ξ_{iK}^{ν} , yielding

$$Q_{iK}^{\nu} = -\frac{\partial \hat{\psi}}{\partial \xi_{iK}^{\nu}} = -\frac{\partial \Upsilon}{\partial \xi_{iK}^{\nu}}.$$
 (4)

Here Q_{iK}^{ν} denotes the viscoelastic stress.⁸ The origin of the work conjugate stress s_{iK} and viscoelastic stress Q_{iK} are determined by combining the first and second laws of thermodynamics. A summary of the thermodynamic framework can be found in.^{8,9} Prior research has extended this framework in the context of both linear and nonlinear viscoelasticity.⁶ The derivation satisfies both first and second laws of thermodynamics, leading to the relation.

$$Q_{iK}^{\nu} = \eta^{\nu} \dot{\xi}_{iK}^{\nu} \tag{5}$$

which is the viscoelastic constitutive law analogous to a spring-dashpot model in one dimension.⁷ We can subsequently use this relationship in our linear viscoelastic model formulation. Moving forward we consider the case where $\nu = 1$ and subsequently remove it from our notation.

2.1 Nonaffine Hyperelastic Model

In conjunction with the viscoelastic model, a nonaffine hyperelastic energy function is implemented 10

$$\psi_{\infty}^{N} = \frac{1}{6}G_c I_1 - G_c \lambda_{max}^2 \ln(3\lambda_{max}^2 - I_1) + G_e \sum_{j} \left(\lambda_j + \frac{1}{\lambda_j}\right),\tag{6}$$

where G_c is the crosslink network modulus, G_e is the plateau modulus, λ_{max} is the maximum stretch of the effective affine tube, and $I_1 = \lambda_i \lambda_i$ is the first stretch invariant where summation on i is implied. Prior research has found this model to yield comparable results to higher order Ogden models, but with fewer phenomenological parameters.⁶

2.2 Linear Viscoelastic Model

In the linear case we hypothesize that the non-conservative energy function has the quadratic form

$$\Upsilon_L = \frac{1}{2} \gamma \left(F_{iK} - \xi_{iK} \right) \left(F_{iK} - \xi_{iK} \right), \tag{7}$$

which leads to the spring-dashpot relation

$$\dot{Q}_{iK} + \frac{1}{\tau} Q_{iK} = \gamma \dot{F}_{iK},\tag{8}$$

where $\tau = \frac{\eta}{\gamma}$.

To reduce the number of terms in the model, we take the rates of the internal state variables to be proportional to the local fractional time derivative of deformation. The details of this fractional derivative can be found in.³ We express this assumption as

$$\dot{\xi}_{iK} = \mu_L D_t^{\alpha} F_{iK},\tag{9}$$

and by using (5) and (9) we obtain

$$Q_{iK} = \eta_L D_t^{\alpha} F_{iK},\tag{10}$$

where $\eta_L = \eta \mu_L$, and D_t^{α} is the fractional time derivative of deformation. For more details regarding the numerical implementation of fractional-order derivatives, the reader is referred to.⁴ The order of the fractional derivative is denoted by α . This is the form of the viscoelastic constitutive law analogous to a spring-dashpot model in the one dimensional fractional model.

2.3 Nonlinear Viscoelastic Model

The nonlinear non-conservative energy function has the form

$$\Upsilon_{NL} = \frac{1}{2} \gamma \xi_{iK} \xi_{iK} - \beta_{\infty} \frac{\partial \psi_{\infty}}{\partial F_{iK}} \xi_{iK} + \beta_{\infty} \psi_{\infty}. \tag{11}$$

A full description of the model derivation and assumptions can be found in.³ Here, we consider the key relationship required for analysis of our nominal stress. The viscoelastic contribution to the nominal stress is found to be

$$\frac{\partial \Upsilon_{NL}}{\partial F_{iK}} = \beta_{\infty} \left[s_{iK}^{\infty} - \frac{\partial s_{iK}^{\infty}}{\partial F_{iK}} \left(\frac{1}{\gamma} (\beta_{\infty} s_{iK}^{\infty} - \eta D_t^{\alpha} s_{iK}^{\infty}) \right) \right]. \tag{12}$$

Here β_{∞}, η , and γ are viscoelastic model parameters, and α is the order of the fractional derivative operator (D_t^{α}) . For details regarding fractional-order operators, please see.^{3,4} A brief description is also provided in Appendix A.

2.4 Model Parameters

When considering sensitivity analysis, we will consider the following sets of parameters. The combined parameter set for the hyperelastic and linear viscoelastic model is

$$\theta_L = [G_c, G_e, \lambda_{max}, \eta, \alpha]. \tag{13}$$

Similarly, when combining the hyperelastic with the nonlinear viscoelastic model we will consider,

$$\theta_{NL} = [G_c, G_e, \lambda_{max}, \eta, \alpha, \gamma, \beta]. \tag{14}$$

3. SENSITIVITY ANALYSIS

Our initial analysis utilizes several methods for performing sensitivity analysis (SA). Each algorithm approaches the problem in a slightly different way, and by comparing the analyses we can gain an overall improved picture of the truly sensitivity components of the model. The constitutive model parameters often vary many orders of magnitude, which can lead to erroneous interpretation of parameter sensitivity. To account for these vary magnitudes, we perform gradient operations in a scaled space, which has been outlined in Section 3.1. We then perform Parameter Subset Selection (PSS) as outlined in Section 3.2 to assess global sensitivity.

3.1 Scaled Gradient Evaluations

To account for vastly different parameter scales, we utilize a scaled gradient method when calculating sensitivity matrices. The basic approach we consider takes all parameters to be uniformly distributed such that

$$\Theta_i \sim \mathcal{U}(\theta_i^{nom} - \delta_i | \theta_i^{nom} |, \theta_i^{nom} + \delta_i | \theta_i^{nom} |). \tag{15}$$

Here, θ_i^{nom} , i=1,...,p, represents the nominal values of the parameters $\boldsymbol{\theta}=[\theta_0,...,\theta_p]$. The value of δ_i is estimated using expert knowledge of parameter variability. To avoid issues associated with differences in units of magnitudes for different sets of parameters, we transform all the distributions in Equation (15) to $\mathcal{U}[0,1]$. The transformation scales all input, while removing units and ensuring that parameters containing relatively large values do not affect the analysis disproportionately. To transform back to the physical input values for the model evaluations, we the use the mapping

$$g_U(\mathbf{x}) = \operatorname{diag}(\theta_u - \theta_l)\mathbf{x} + \theta_l, \tag{16}$$

where x is a p-vector with values between 0 and 1, and θ_l and θ_u are the vectors with the lower and upper bounds of the parameters θ . Note that in our problem, the upper and lower bound vectors are

$$\theta_l = \boldsymbol{\theta}^{nom} - \delta_i |\boldsymbol{\theta}^{nom}| \text{ and } \boldsymbol{\theta}_u = \boldsymbol{\theta}^{nom} + \delta_i |\boldsymbol{\theta}^{nom}|$$
 (17)

where $\boldsymbol{\theta}^{nom}$ is the vector of nominal values for the parameters.

3.2 Quasi-Global Parameter Subset Selection (PSS)

The PSS serves as a means of reducing the number of parameters in the calibration by systematically comparing the eigenvalues of the Fisher Information matrix with respect to some threshold. The details of PSS are summarized in Algorithm 3.1, and more details can be found in.¹¹ Within the PSS algorithm, we consider a sensitivity matrix of the form

$$S = \begin{bmatrix} \frac{\partial f}{\partial \theta_1} \left(x_1^1; \theta^* \right) & \cdots & \frac{\partial f}{\partial \theta_p} \left(x_1^1; \theta^* \right) \\ \vdots & & \vdots \\ \frac{\partial f}{\partial \theta_1} \left(x_1^N; \theta^* \right) & \cdots & \frac{\partial f}{\partial \theta_p} \left(x_1^N; \theta^* \right) \end{bmatrix}, \tag{18}$$

where θ^* is a nominal set of parameter values, and f is the model for our quantity of interest (QoI). To account for variability in the parameter space, we propose a methodology that explores the space of θ to obtain a measure for global sensitivity, while employing the underlying theory behind Algorithm 3.1.

Algorithm 3.1: Parameter subset selection algorithm to determine locally unidentifiable parameters. 12

- (0) Set $\eta = p$, where p is the number of parameters in the model, and construct the sensitivity matrix S following relation (18). We note that the variable η changes with the iterations of the algorithm.
- (1) Compute the matrix S^TS and its eigenvalues, and order their magnitudes as

$$|\lambda_1| \leq |\lambda_2| \leq \cdots \leq |\lambda_n|$$
.

- (2) If $|\lambda_1| > \epsilon$, where ϵ is some prescribed threshold value, stop. We take all the parameters to be identifiable.
- (3) If $|\lambda_1| < \epsilon$, then one of the parameters is not identifiable. Proceed as follows.
- (4) Identify the component with the largest magnitude in the eigenvector $\Delta\theta_1$ associated with λ_1 . This component corresponds to the least identifiable parameter.
- (5) Remove the column in S corresponding to the component identified in Step 4, set $\eta = \eta 1$ and repeat Step 1.

To construct a quasi-global sensitivity matrix, we use a method similar to Morris screening. 13 We obtain the elementary effects

$$s_{ij}^{\ell} = \frac{\partial f}{\partial \theta_{i}}(x_{1}^{j}; \theta^{\ell}), \ \ell = 1, \dots, K,$$

$$s_{ij}^{\ell} = \frac{f(x_{1}^{i}; \theta_{1}^{\ell}, \dots, \theta_{j-1}^{\ell}, \theta_{j}^{\ell} + \Delta, \theta_{j+1}^{\ell}, \dots, \theta_{p}^{\ell}) - f(x_{1}^{i}; \theta^{\ell})}{\Delta}$$

$$= \frac{f(x_{1}^{i}; \theta^{\ell} + \Delta \cdot \mathbf{e}_{j}) - f(x_{1}^{i}; \theta^{\ell})}{\Delta},$$
(19)

where Δ is the step size and \mathbf{e}_j is the j^{th} canonical vector. We evaluate these effects via a sampling procedure which reflects the uncertainty in the parameter values. We average over all the sampled sensitivity entries to obtain the sensitivity measures

$$s_{ij}^* = \frac{1}{K} \sum_{\ell=1}^K s_{ij}^{\ell}.$$

This provides a quasi-global sensitivity matrix

$$S^* = \begin{bmatrix} s_{11}^* & \cdots & s_{1p}^* \\ \vdots & & \vdots \\ s_{N1}^* & \cdots & s_{Np}^* \end{bmatrix}. \tag{20}$$

We employ this quasi-global sensitivity matrix along with Algorithm 3.1 for the parameter subset selection investigation in this paper.

3.3 Results

We generate a global sensitivity matrix for the linear and nonlinear viscoelastic model by sampling 2000 times throughout the parameter space, calculating a local sensitivity matrix, and then average to estimate a global approximation. The global estimate was then used in the parameter subset selection algorithm to identify the sensitive parameters in the model. From the first iteration of the PSS algorithm, we observe the eigenvalues of the Fisher information matrix, shown in Figure 1. The results of our PSS are presented in Tables 1 and 2 for the linear and nonlinear model, respective. We have shown the minimum magnitude eigenvalue at each iteration as well as the corresponding eigenvector components.

For the linear viscoelastic model, the PSS algorithm removed parameters in the order G_e , η , α . However, in light of the relative eigenvalue spectra observed in Figure 1(a), none of the jumps in eigenvalues is significant enough to justify removing parameters from calibration. In contrast, when considering the nonlinear viscoelastic model, the PSS algorithm removed parameters in the following order: γ , η , and G_e . Based on the results of the PSS and in light of the differences observed in the eigenvalues in Figure 1(b), we conclude that γ is non-influential. The noticeable jump between the 6^{th} and 7^{th} eigenvalues indicate that the last parameter is significantly less influential than the other terms. With this information, we will perform parameter estimation for the linear set

$$\theta_{FOV}^{s1} = [G_c, G_e, \lambda_{max}, \eta, \alpha, \beta], \tag{21}$$

and leave the nonlinear set for future work

$$\theta_{FOV}^{s2} = [G_c, \lambda_{max}, \alpha, \beta]. \tag{22}$$

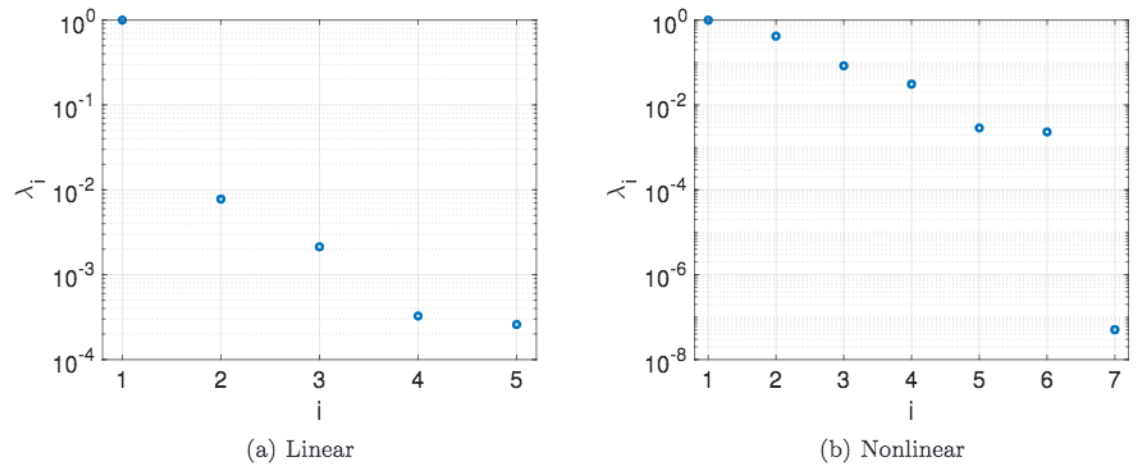


Figure 1. Eigenvalues from first iteration of PSS algorithm.

Table 1. Results from Algorithm 3.1 with the quasi-global sensitivity matrix to determine noninfluential parameters in θ_L .

		Eigenvector $\Delta \theta_1$ with corresponding parameters									
Iteration	$ \lambda_1 $	G_c	G_e	λ_{max}	η	α					
1	2.54e-04	-1.69e-01	9.02e-01	-3.95e-01	-3.27e-02	-1.09e-02					
2	3.33e-04	-8.00e-03		1.86e-02	-8.52e-01	-5.23e-01					
3	1.66e-03	1.67e-02	_	-8.83e-02	_	9.96e-01					
4	$5.85\mathrm{e}\text{-}03$	-1.83e-01	_	-9.83e-01		_					
Result: All parameters are influential.											

Table 2. Results from Algorithm 3.1 with the quasi-global sensitivity matrix to determine noninfluential parameters in θ_{NL} .

		Eigenvector $\Delta\theta_1$ with corresponding parameters									
Iteration	$ \lambda_1 $	G_c	G_e	λ_{max}	η	α	γ	β			
1	3.12e-08	-2.54e-01	-2.53e-01	1.23e-03	5.27e-01	-1.20e-04	5.49e-01	5.40e-01			
2	2.23e-03	-4.61e-01	-2.42e-01	-8.60e-02	8.49e-01	-1.85e-02	_	-2.34e-02			
3	4.47e-03	-2.38e-01	9.16e-01	-3.11e-01		-8.71e-02		-4.53e-03			
4	$4.62\mathrm{e}\text{-}02$	8.99e-02	_	-9.12e-01	_	1.10e-01	_	-3.86e-01			
Result: The parameter γ is not influential.											

4. MODEL CALIBRATION

We calibrate the remaining influential parameters by employing the Bayesian techniques detailed in.^{3,5,6} This calibration serves two purposes: (1) construct marginal densities for the input parameters and thus characterize inherent uncertainties, and (2) produce pairwise correlation plots to assess parameter identifiability. We consider all five parameters from the linear model, namely the set (21). Note that this set is the same as the calibration in³ with a Riemann-Liouville implementation for the fractional time derivative instead of a Caputo definition. We calibrate the model with respect to stretch-stress data collected at a stretch rate of 6.7×10^{-5} Hz for the dielectric elastomer Very High Bond (VHB) 4910 (made by 3M). For more details regarding the experimental data collection, please see.⁶ The calibration is performed using the Delayed Rejection Adaptive Metropolis (DRAM) algorithm, ¹⁴ and the resulting chains are presented in Figure 2.

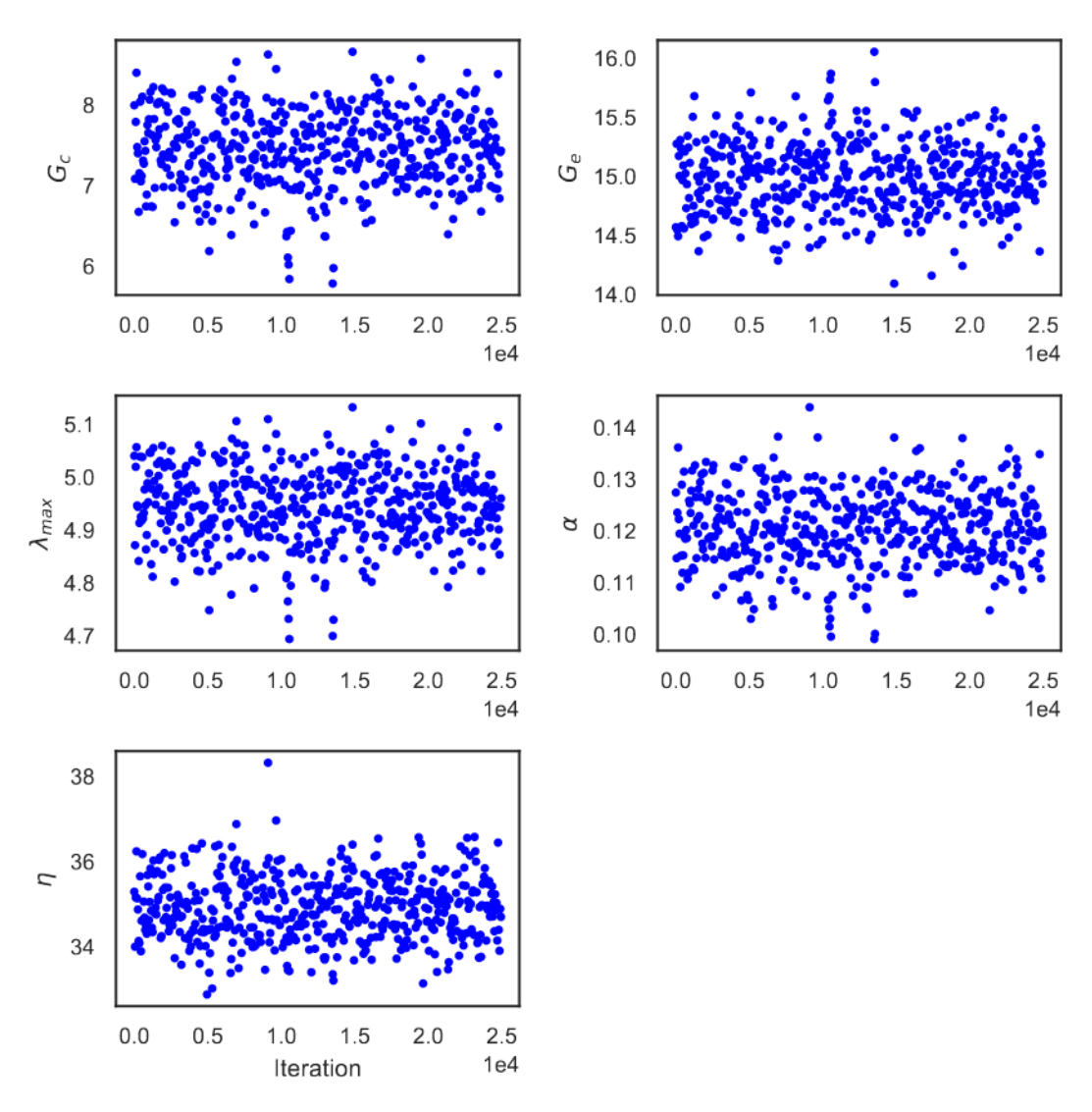


Figure 2. Sampling history from calibration of linear viscoelastic model.

We conclude that the marginal paths have converged qualitatively by observing that the appearance of each chain being analogous to white noise with no significant jumps in mean behavior or stagnation regions. Rigorous statistical convergence tests are discussed in. ^{14–16} With chains that have converged to the fixed posterior distribution, we construct marginal densities with a kernel density estimate (KDE) algorithm and present these

densities along the main diagonal of Figure 3. We note that many of the parameters appear to have qualitatively converged to a Gaussian distribution; however, that is not required by the algorithm. To verify whether or not the posteriors are actually normally distributed, we could plot the chains on a Q-Q plot, but it is not important for the current analysis.

Another feature of the calibration process is an indication of potential parameter correlation. This is visualized in the off-diagonal elements of Figure 3. In the upper-triangular elements, we observe pairwise correlation plots, and in the lower-triangular elements we see the corresponding two-dimensional posterior distribution. Figure 3 reveals significant correlation structure between several parameters, including the fractional order. This is understandable, as the fractional order of the derivative affects the entire model response for a given set of physical parameters. Correlated parameters is a perfectly valid outcome of the calibration, and in this case none of the parameter correlations appear to be single-valued. This supports the conclusion that all the parameters in (21) were significant, and in this case were identifiable given the data used to calibrate.

5. CONCLUDING REMARKS

In this paper we have shown how global parameter subset selection (PSS) can be used to identify the most sensitive parameters in a linear and nonlinear viscoelastic model. These results can then be used to help determine which parameters to include in model calibration with respect to data. We note that for the models presented here, the relative eigenvalue spectra of the linear viscoelastic model in conjunction with hyperelasticity revealed all five model parameters to be important. However, when considering the nonlinear model, we observe a significant jump for the last eigenvalue, and conclude that the parameter γ can be fixed a nominal value for subsequent calibration. Calibration results are presented for the linear viscoelastic model, showing that all parameter distributions were identifiable, support the conclusion of the GSA. Calibrating the nonlinear viscoelastic model is left as future work.

ACKNOWLEDGMENTS

P.M., G.P. and R.S. thank the support provided by AFOSR FA9550-15-1-0299. G.P was supported in part by the National Science Foundation (NSF) award DMS-1745654. Any opinions, findings, and conclusions or recommendations expressed in this publication are those of the authors and do not necessarily reflect the views of the funding sponsors.

APPENDIX A. NUMERICAL METHODS

For more details regarding the numerical implementation, the reader is referred to.⁴ A few key definitions are provided below for clarity. Note that for our analysis we consider the Riemann-Liouville definition for fractional derivatives¹⁹

$$D_{RL}^{\alpha}[f(t)] = \frac{1}{\Gamma(n-\alpha)} \frac{d^n}{dt^n} \int_0^t \frac{f(s)}{(t-s)^{\alpha+1-n}} ds, \tag{23}$$

where $n = \lceil \alpha \rceil$. We will restrict our analysis further by only considering the regime where $\alpha \in [0,1)$; therefore n = 1, and the definition simplifies to

$$D_{RL}^{\alpha}[f(t)] = \frac{1}{\Gamma(1-\alpha)} \frac{d}{dt} \int_0^t \frac{f(s)}{(t-s)^{\alpha}} ds.$$
 (24)

Gaussian Quadrature, Riemann-Sum (GQRS)

The challenge that arises in evaluating the fractional derivative is the singularity that occurs at the right end point. However, many quadrature methods are suitable for evaluating the integral over regions reasonably far away from the singularity. As an optimal approach we consider using Gaussian Quadrature (GQ) in regions far from the singularity and estimate near the singularity using a Riemann-Sum (RS) approximation. For more

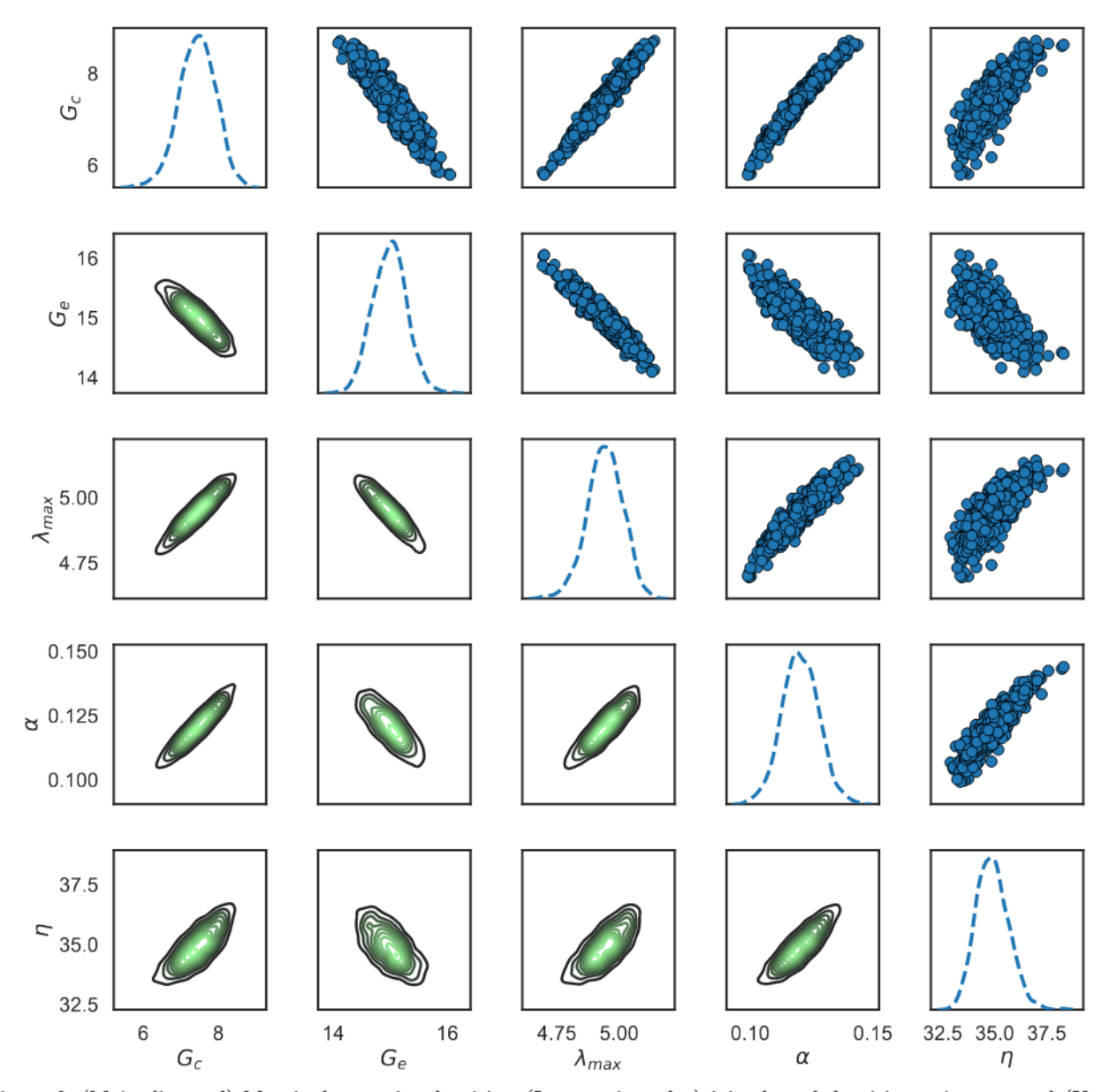


Figure 3. (Main diagonal) Marginal posterior densities, (Lower triangular) joint kernel densities estimates, and (Upper triangular) pairwise correlation. Plot made using. 17, 18

details regarding GQ and RS the reader is referred to.^{4,20} This is accomplished by breaking the integral into two parts:

$$\int_{a}^{b} \frac{f(s)}{(t-s)^{\alpha}} ds = \underbrace{\int_{a}^{b-b_{T}} \frac{f(s)}{(t-s)^{\alpha}} ds}_{\text{GQ}} + \underbrace{\int_{b-b_{T}}^{b} \frac{f(s)}{(t-s)^{\alpha}} ds}_{\text{RS}},$$
(25)

where $b_T = \phi(b-a)$. We can adjust the portion of the integral solved via GQ and that using the RS approach by specifying different values for ϕ . For example, we consider the case where $\phi = 0.05$ which means that 95% of the interval is approximated using GQ, and the remaining 5% is approximated using a reasonable number of terms in our RS method.

REFERENCES

- Bergström, J. and Boyce, M., "Constitutive modeling of the large strain time-dependent behavior of elastomers," Journal of the Mechanics and Physics of Solids 46(5), 931-954 (1998).
- [2] Holzapfel, G. A., "On large strain viscoelasticity: continuum formulation and finite element applications to elastomeric structures," *International Journal for Numerical Methods in Engineering* 39(22), 3903–3926 (1996).
- [3] Mashayekhi, S., Miles, P., Hussaini, M. Y., and Oates, W. S., "Fractional viscoelasticity in fractal and non-fractal media: Theory, experimental validation, and uncertainty analysis," *Journal of the Mechanics* and Physics of Solids 111, 134–156 (2018).
- [4] Miles, P., Pash, G., Oates, W., and Smith, R. C., "Numerical techniques to model fractional-order nonlinear viscoelasticity in soft elastomers," in [ASME 2018 Conference on Smart Materials, Adaptive Structures and Intelligent Systems], V001T03A021, American Society of Mechanical Engineers (2018).
- [5] Smith, R. C., [Uncertainty Quantification: Theory, Implementation, and Applications], Society for Industrial and Applied Mathematics, Philadelphia, PA, USA (2014).
- [6] Miles, P., Hays, M., Smith, R., and Oates, W., "Bayesian uncertainty analysis of finite deformation viscoelasticity," Mechanics of Materials 91, 35–49 (2015).
- [7] Holzapfel, G. A., [Nonlinear solid mechanics], vol. 24, Wiley Chichester (2000).
- [8] Holzapfel, G. A. and Simo, J. C., "A new viscoelastic constitutive model for continuous media at finite thermomechanical changes," *International Journal of Solids and Structures* 33(20), 3019–3034 (1996).
- [9] Peng, S., Valanis, K., and Landel, R., "Nonlinear viscoelasticity and relaxation phenomena of polymer solids," Acta Mechanica 25(3-4), 229-240 (1977).
- [10] Davidson, J. D. and Goulbourne, N., "A nonaffine network model for elastomers undergoing finite deformations," Journal of the Mechanics and Physics of Solids 61(8), 1784–1797 (2013).
- [11] Leon, L., Smith, R. C., Oates, W. S., and Miles, P., "Analysis of a multi-axial quantum-informed ferroelectric continuum model: Part 2sensitivity analysis," *Journal of Intelligent Material Systems and Structures* 29(13), 2840–2860 (2018).
- [12] Quaiser, T. and Mönnigmann, M., "Systematic identifiability testing for unambiguous mechanistic modeling–application to jak-stat, map kinase, and nf- κ b signaling pathway models," *BMC systems biology* **3**(1), 50 (2009).
- [13] Morris, M. D., "Factorial sampling plans for preliminary computational experiments," Technometrics 33(2), 161–174 (1991).
- [14] Haario, H., Laine, M., Mira, A., and Saksman, E., "Dram: efficient adaptive mcmc," Statistics and computing 16(4), 339–354 (2006).
- [15] Haario, H., Saksman, E., Tamminen, J., et al., "An adaptive metropolis algorithm," *Bernoulli* 7(2), 223–242 (2001).
- [16] Gelman, A., Stern, H. S., Carlin, J. B., Dunson, D. B., Vehtari, A., and Rubin, D. B., [Bayesian data analysis], Chapman and Hall/CRC (2013).
- [17] Waskom, M., Botvinnik, O., O'Kane, D., Hobson, P., Ostblom, J., Lukauskas, S., Gemperline, D. C., Augspurger, T., Halchenko, Y., Cole, J. B., Warmenhoven, J., de Ruiter, J., Pye, C., Hoyer, S., Vanderplas, J., Villalba, S., Kunter, G., Quintero, E., Bachant, P., Martin, M., Meyer, K., Miles, A., Ram, Y., Brunner, T., Yarkoni, T., Williams, M. L., Evans, C., Fitzgerald, C., Brian, and Qalieh, A., "mwaskom/seaborn: v0.9.0 (july 2018)," (July 2018).
- [18] Miles, P., "prmiles/mcmcplot: v0.0.0," (Aug. 2018).
- [19] Podlubny, I., [Fractional differential equations: an introduction to fractional derivatives, fractional differential equations, to methods of their solution and some of their applications], vol. 198, Academic press (1998).
- [20] Smith, R. C., [Smart material systems: model development], vol. 32, SIAM, Philadelphia, PA (2005).